*Korean J. of Chem. Eng.*, **14**(4), 277-284 (1997)

# EFFECT OF OPERATING CONDITIONS ON ADSORPTION OF CEPHALOSPORIN C IN A COLUMN ADSORBER

**Jae Wook Lee†, Heung Joe Jung and Hee Moon***

Department of Chemical Engineering, Seonam University, Namwon 590-170, Korea
*Department of Chemical Technology, Chonnam National University, Kwangju 500-757, Korea
*(Received 6 March 1997 • accepted 30 June 1997)*

**Abstract** – Adsorption of cephalosporin C on a non-ionic polymeric sorbent, SP850, was studied in a column adsorber under various operating conditions such as temperature, pH, concentration, flow rate, and L/D ratio. An adsorption model was formulated by employing the surface diffusion inside resin particles. Single-species equilibrium data were simply represented by Freundlich equation. The model equations were solved numerically by an orthogonal collocation method. The model successfully simulates the adsorption behavior in a column under different operating conditions, but the considerable deviations are observed at low solution pHs, at which different ionic species may coexist.

*Key words: Adsorption, Cephalosporin C, Column Adsorber, Nonionic Polymeric Sorbent, Operating Conditions*

## INTRODUCTION

Antibiotics can be generally classified such as β-lactam, aminoglycoside, macrolide, peptide, polyether, etc., according to the physical and chemical properties. Nowadays, β-lactam has occupied about 70% in the worldwide antibiotic market. Among β-lactam antibiotics, especially, the demand for cephems has increased rapidly because of great stability in acid and activity rather than penems [Smith, 1985]. Cephalosporin C, one of the cephems, produced by *cephalosporium acremonium* has been widely used as an important starting material to make medical and pharmaceutical products. Although its antibacterial activity is low and similar in range to that of penicillin N, cephalosporin C unlike the penicillin N is not hydrolyzed by a penicillinase [Abraham, 1986; Elander and Aoki, 1982]. Hence it has a potential clinical interest. The key process for the production of cephalosporin C is the question of separation and purification from its fermentation broths that contained many components such as cephalosporin C, deacetoxycephalosporin C, penicillin N, methionine and its decomposition product, 2-hydroxy-4-methylmercaptobutyric acid etc. [Abraham, 1986; Elander and Aoki, 1982].

Liquid chromatography and adsorption processes have been employed extensively in large scale for biochemical recovery and purification [Asenjo, 1983; Belter et al., 1988; Dechow, 1989; Wankat, 1980]. Adsorption techniques for the separation and purification of cephalosporin C have been widely used because the nature of α-aminoadipyl side chain of cephalosporin C is hydrophilic. Although nonionic polymeric sorbents have lower adsorption capacity for cephalosporin C than ionic exchanger and activated carbon, they have been used due to the relatively more easy elution and regeneration steps on an industrial cyclic operation [Nara et al., 1975]. A cycle involves three main steps; adsorption, desorption and washing. When and how the breakthrough occurs is an important task for the designing, optimization and scale-up of column adsorbers. Therefore, the simulation of such a cycle operation needs a mathematical model for each step. The model can be formulated on the basis of conservation equations in the column, mass transport within the resin particles, and equilibrium relationship at the liquid-solid interface. The model parameters such as equilibrium data, film mass transfer coefficient, intraparticle diffusivity, and axial dispersion coefficient can be measured experimentally, or predicted by existing correlation, or optimized from experimental data [Costa and Rodriques, 1985]. In general, the constructed model equations with nonlinear adsorption isotherm can not be solved analytically. Therefore, a numerical solution should be devised. A finite difference method or an orthogonal collocation method have been generally used for the simulation of the transient response of an adsorption column.

The shape and width of the breakthrough curve are crucially important in the designing of adsorbers for a cyclic separation process. The breakthrough curve generally depends on the adsorption isotherm and the transport mechanisms in sorbent particles as well as in operating conditions of the column. In order to device the separation and purification method of cephalosporin C from its fermentation broths, it is essential to get information, in advance, about the adsorption behavior of pure cephalosporin C in a column adsorber. In the previous work, we selected a proper resin, SP850, for adsorption of cephalosporin C among three nonionic polymer resins, SP207, SP850 and XAD-2, in terms of adsorption capacity and desorption characteristics. This paper presents the dynamic behavior of cephalosporin C in the column adsorber charged with SP850 under various operating conditions as a continuous work. The adsorption dynamic model which employs the surface diffusion [Moon and Lee, 1983;

†To whom all correspondence should be addressed.

Moon and Tien, 1987] for intraparticle mass transfer combined with the Freundlich equation for single-species equilibrium was successfully used to simulate the experimental breakthrough curves measured under various operating conditions such as temperature, pH, concentration, flow rate and L/D ratio. The approach used here will serve as a useful tool for designing, optimization, and scale-up of the column adsorber for the direct separation and purification of cephalosporin C from its fermentation broths.

## THEORETICAL APPROACH

### 1. Dynamic Model Description Based on Surface Diffusion

To formulate a dynamic model, we made the following assumptions: (1) homogeneous packing; (2) plug flow with a constant linear velocity along the column; (3) isothermal adsorption column; (4) homogeneous pore size distribution; (5) constant surface diffusivities within the adsorbent; (6) local equilibrium. Under these assumptions, the transport equation inside a spherical adsorbent particle may be described by the following equation:

$$\frac{\partial q_i}{\partial t} = D_{si}\left(\frac{\partial^2 q_i}{\partial r^2} + \frac{2}{r}\frac{\partial q_i}{\partial r}\right) \tag{1}$$

with the initial and boundary conditions:

$$q_i(r,\ t=0)=0 \tag{2}$$

$$\left.\frac{\partial q_i}{\partial r}\right|_{r=0} = 0 \tag{3}$$

$$D_{si}\rho_p \left.\frac{\partial q_i}{\partial r}\right|_{r=R} = k_f(C_i - C_{si}) \tag{4}$$

The mass balance equation in the column and the relevant initial and boundary conditions are:

$$-D_L\frac{\partial^2 C_i}{\partial z^2} + \frac{\partial vC_i}{\partial z} + \frac{\partial C_i}{\partial t} + \frac{1-\varepsilon_b}{\varepsilon_b}\frac{3}{R}(C_i - C_{si}) = 0 \tag{5}$$

$$C_i(z,\ t=0)=0 \tag{6}$$

$$D_L\left.\frac{\partial C_i}{\partial z}\right|_{z=0} = -v(C_i|_{z=0^-} - C_i|_{z=0^+}) \tag{7}$$

$$\left.\frac{\partial C_i}{\partial z}\right|_{z=L} = 0 \tag{8}$$

The above set of equations can be rendered dimensionless as follows:

$$\frac{\partial \Psi_i}{\partial \tau} = \gamma_i\left(\frac{\partial^2 \Psi_i}{\partial X^2} + \frac{2}{X}\frac{\partial \Psi_i}{\partial X}\right) \tag{9}$$

$$\Psi_i(X,0)=0 \tag{10}$$

$$\left.\frac{\partial \Psi_i}{\partial X}\right|_{X=0} = 0 \tag{11}$$

$$\left.\frac{\partial \Psi_i}{\partial X}\right|_{X=1} = \beta_i\lambda_i(\xi_i - \xi_{si}) \tag{12}$$

$$\frac{\partial \xi_i}{\partial \tau} - \frac{1}{Pe}\frac{\partial^2 \xi_i}{\partial Z^2} + \frac{\partial \xi_i}{\partial Z} + 3\mu(\xi_i - \xi_{si}) = 0 \tag{13}$$

$$\xi_i(Z,\ \tau=0)=0 \tag{14}$$

$$-\left.\frac{\partial \xi_i}{\partial Z}\right|_{Z=0} = -Pe(\xi_i|_{Z=0^-} - \xi_i|_{Z=0^+}) \tag{15}$$

$$\left.\frac{\partial \xi_i}{\partial Z}\right|_{Z=1} = 0 \tag{16}$$

The dimensionless variables have already been listed in details in our previous report [Lee et al., 1997].

### 2. Numerical Method

All the parabolic second-order partial differential equations, Eqs. (9) and (13), can not be solved analytically. Therefore, a numerical method must be employed. In this work, we used a numerical solution techniques, which transforms all PDE's into a system of ordinary equations using an orthogonal collocation method [Carey and Finlayson, 1975] with several interior collocation points;

$$\frac{\partial \Psi_i^{(k)}}{\partial \tau} = \gamma^{(k)}\left\{\sum_{j=1}^{NTS-1}\frac{2}{X_i}\left(AS_{i,j} - \frac{AS_{i,NTS}AS_{NTS,j}}{AS_{NTS,NTS}}\right)\Psi_j^{(k)} + \sum_{j=1}^{NTS-1}\left(BS_{i,j} - \frac{BS_{i,NTS}AS_{NTS,j}}{AS_{NTS,NTS}}\right)\Psi_j^{(k)} + \frac{\left(BS_{i,NTS} + \frac{2}{X_i}AS_{i,NTS}\right)}{AS_{NTS,NTS}}\beta_j\lambda_i\left(\xi^{(k)} - \xi^{(sk)}\right)\right\} \tag{17}$$

$$\frac{\partial \xi_l^{(k)}}{\partial \tau} = \frac{\alpha}{Pe}\sum_{j=1}^{NTF}BF_{l,j}\xi_j^{(k)} - \alpha\sum_{j=1}^{NTF}AF_{l,j}\xi_j^{(k)} - 3\mu(\xi^{(k)} - \xi^{(sk)}) \tag{18}$$

where i,j and *l*,j are the collocation numbers in the particle and along the column, respectively. The surface concentration, $\xi^{(sk)}$, can be determined from the corresponding isotherm or equilibrium theories [Myers and Prausnitz, 1965]. Inserting the surface concentration term into Eqs. (17) and (18), these ordinary differential equations of two vectors, $\frac{\partial \xi_i^{(k)}}{\partial \tau}$ and $\frac{\partial \Psi_l^{(k)}}{\partial \tau}$, are simultaneously integrated with respect to $\tau$ by using the integrating package, DGEAR. DGEAR employs the variable-step size, variable-order, and predictor-corrector techniques that are suitable for stiff equations.

## EXPERIMENTAL

The nonionic polymeric sorbent used in this study was a macroreticular and spherical sulfonated polystyrene resin cross-linked with DVB (divinylbenzene), SP850, manufactured by

**Table 1. Properties of a polymeric sorbent, SP850**

| Property | Values | Unit |
|---|---|---|
| Particle diameter | 382 | μm |
| Particle density | 457 | $kg/m^3$ |
| Moisture content* | 52 | % |
| Surface area* | 1,000 | $m^2/g$ |
| Average pore diameter* | 38.1 | A |
| Pore volume* | 0.89 | ml/g |

*From the manufacturer's report.

**Table 2. Properties of cephalosporin C**

| Property | | Values |
|---|---|---|
| Chemical formula | | $C_{16}H_{21}N_3O_8S$ |
| MW | | 415.44 |
| Analysis (UV) | | 260 |
| pKa | about | 2.6, 3.1, 9.8 |

Mitzubishi Co. (Japan). The physical properties of SP850 are summarized in Table 1. The arithmetic average particle diameter was determined by sorting wet resin particles with the aid of an optical microscope. The average size was estimated to be 382 μm.

The β-lactam antibiotics studied in this work was cephalosporin C as a zinc form (Sigma, U.S.A.) used for a standard material, and with a sodium form (Cheil Food & Chemicals Inc., Korea) for experimental use. The properties of cephalosporin C are listed in Table 2. Both cephalosporin C were used without further purification. HCl and NaOH solutions were used to adjust solution pH. The concentrations of cephalosporin C in aqueous solutions were determined using a spectrophotometer (Varian, model DMS 100S) at 260 nm. All chemicals used were of analytical reagent grade and distilled, deionized water was used to prepare all stock solutions.

Prior to experiments, the sorbent was leached with isopropyl alcohol for 24 hrs to wet internal pores. Sorbent particles were loaded in a 0.02 m ID glass column and a ten-bed volume of sodium hydroxide (0.1 N) and HCl (0.1 N), respectively, was passed through the column at a flow rate of $1.0\times10^{-4}$ $m^3/min$ in order to rinse the impurities. Then, a twenty bed-volume of distilled and deionized water was passed at the same flow rate to remove the HCl.

Equilibrium data were taken by introducing a given amount of sorbent into a mixed solution with an excess volume, 50 ml, of a cephalosporin C solution containing 1-100 $mol/m^3$ at two temperatures (278.15, 298.15 K) and three pHs (3.40, 5.30, 7.50), while shaking in a constant temperature incubator. The dry-base weight of sorbent was measured by weighing after drying for 48 hours in a vacuum oven at 353.15 K. After equilibrium was reached, the excess cephalosporin C left in solutions was analyzed by using UV. The adsorption capacity of the resin was determined from material balance.

Single-species adsorption was carried out in a column adsorber which was made of a glass column of 0.02 m diameter and 0.15 m length. The column was lined with a water jacket to maintain the uniform column temperature. The flow rate was regulated by a precision FMI pump (model RHOCKE). The solution was introduced downward into the column. To prevent channeling and to enhance distribution of the solution through the column, the two layers of small glass beads were packed in the top and bottom region of the column. Various breakthrough experiments were carried out under experimental conditions listed in Table 3. The samples were withdrawn from the effluent line and analyzed using a UV spectrophotometry.

**Table 3. Experimental conditions for fixed-bed adsorption**

| Variables | Range | Unit |
|---|---|---|
| Bed length (L) | 0.05-0.44 | m |
| Bed diameter (D) | 0.01-0.02 | m |
| Flow rate (v) | $0.50\text{-}2.12\times10^{-4}$ | m/sec |
| Bed porosity ($\varepsilon_b$) | 0.37 | - |
| Packing density ($\rho_b$) | 290 | $kg/m^3$ |
| Temperature (T) | 278.15, 298.15 | K |
| pH | 2.5-8.0 | - |
| Cephalosporin C conc. | 1-100 | $mol/m^3$ |

## RESULTS AND DISCUSSION

### 1. Adsorption Isotherms in Terms of Temperature and pH

Adsorption onto a synthetic polymeric sorbents is mainly driven by physical sorption in the range of the van der Waals' force working between the adsorbate and the resin. Therefore, the adsorption capacity highly depends on the chemical structure of the adsorbate, temperature and solution pH.

Figs. 1 and 2 show the adsorption capacity of pure cephalosporin C in terms of temperature and pH. These isotherm data were obtained at various temperatures and solution pHs up to the concentration range of 100 $mol/m^3$ since the concentration of cephalosporin C is in the range of 50-70 $mol/m^3$ in its actual fermentation broths. The adsorption amounts decreased with temperature and pH. When compared with temperature, it was observed that pH affected more strongly

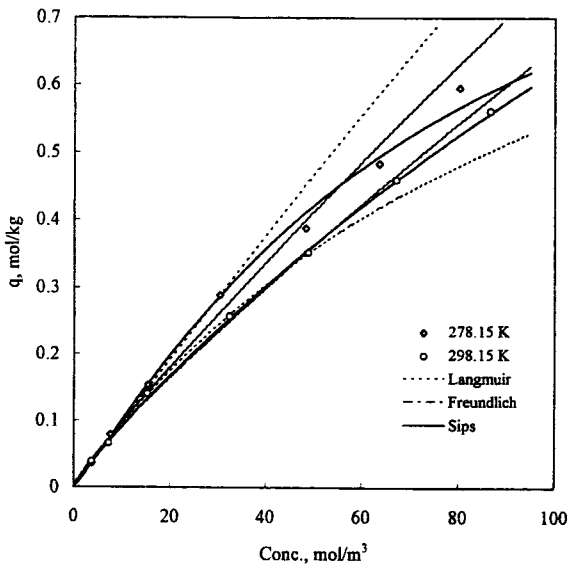


**Fig. 1. Adsorption equilibrium of cephalosporin C on SP850 at pH 5.30.**

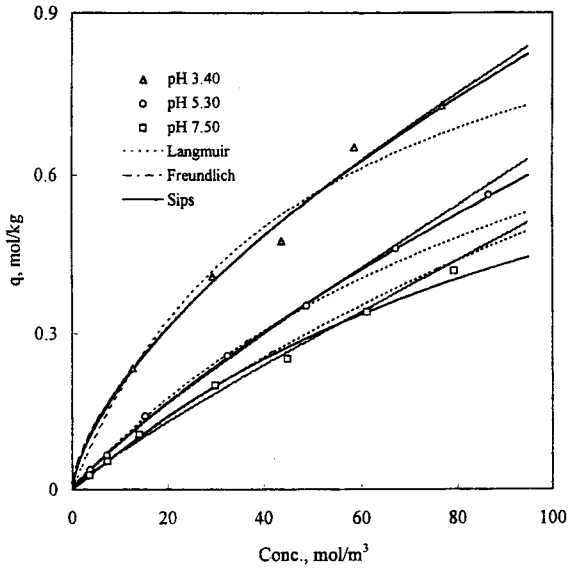


**Fig. 2. Adsorption equilibrium of cephalosporin C on SP850 at 298.1 K.**

on the adsorption capacity of cephalosporin C on SP850. This implies that the effective separation and purification could be achieved by adjustment of the solution pH rather than temperature from the engineering point of view.

Single-species isotherm data were correlated by a well-known two-parameter isotherms such as Langmuir and Freundlich equations and a three-parameter one, Sips equation. We obtained the isotherm parameters by minimizing the mean percent deviation between experimental and predicted amount adsorbed.

$$E(\%) = \frac{100}{N}\sum_{i=1}^{N}\left(\frac{|q_{exp} - q_{pre}|}{q_{exp}}\right)_i \quad (19)$$

As shown in Table 4, the deviations are almost same. It is quite natural that the Sips equation is better than the Freundlich equation to represent single-species equilibrium data. However, we selected the Freundlich equation due to its simplicity (two parameters). This will reduce calculation times for simulating breakthrough curves.

**2. Determination of Model Parameters**

In columns packed with porous adsorbents, the main parameters for the transport of adsorbates are the axial dispersion coefficient, the external film mass transfer coefficient, and the intraparticle diffusion coefficient.

**Table 4. Adsorption equilibrium constants of cephalosporin C on SP850**

| pH | Temp. | Langmuir | | Freundlich | | Sips | | |
|---|---|---|---|---|---|---|---|---|
| | [K] | $q_m$ | b | k | n | $q_m$ | b | n |
| 3.40 | 298.15 | 1.093 | 0.021 | 0.046 | 1.572 | 6.630 | 0.006 | 1.469 |
| E(%) | | 5.709 | | 3.306 | | 4.081 | | |
| 5.30 | 298.15 | 1.140 | 0.009 | 0.013 | 1.163 | 3.070 | 0.004 | 1.090 |
| E(%) | | 3.862 | | 3.097 | | 2.003 | | |
| 7.50 | 298.15 | 1.577 | 0.005 | 0.009 | 1.138 | 0.920 | 0.008 | 0.950 |
| E(%) | | 4.147 | | 5.397 | | 3.132 | | |
| 5.30 | 278.15 | 9.804 | 0.001 | 0.012 | 1.107 | 1.110 | 0.008 | 0.889 |
| E(%) | | 10.188 | | 6.958 | | 3.379 | | |

Axial dispersion contributes to the broadening of the adsorption front due to flow in the interparticle void spaces. Usually it comes from the contribution of molecular diffusion and the dispersion caused by fluid flow. A correlation suggested by Wakao and Funazkri [1978] has been used successfully for liquid-phase systems.

$$D_L = \left(\frac{20}{Re\,Sc} + \frac{1}{2}\right)2vR \quad (20)$$

For spherical particles, the external film mass transfer coefficient, $k_f$, in columns, have been correlated by the Ranz and Marshall equation [Ruthven, 1984].

$$2k_fR/D_m = 2.0 + 0.6Sc^{1/3}Re^{1/2} \quad (21)$$

where Sc and Re mean Schmidt and Reynolds numbers, respectively. Molecular diffusion coefficients, $D_m$, of cephalosporin C in water estimated by the Wilke-Chang equation [Reid, 1994]. Under the experimental conditions used here, the axial dispersion coefficient estimated was $1.0\text{-}2.0\times10^{-6}$ $m^2$/sec. The external film mass transfer coefficient is in the range of $1.05\text{-}1.30\times10^{-5}$ m/sec.

Rate of adsorption in porous adsorbents are generally controlled by transport within the particle, rather than by the intrinsic kinetics of sorption at the surface. Although there are various methods for determining the diffusion coefficient in the literature, the general method for the estimation of diffusion coefficients within the particle was determined by comparing the experimental concentration history and the predicted one based on diffusion model. As shown in Fig. 3, the effective surface diffusion coefficients of cephalosporin C in SP850 were determined from experimental breakthrough curves by minimizing the object function defined in Eq. (19). The values of $D_s$ under our experimental conditions were ap-

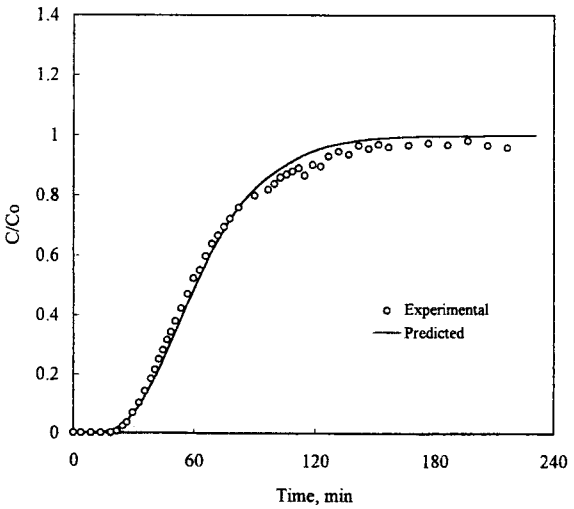


**Fig. 3. Experimental and predicted breakthrough curves of cephalosporin C on SP850 (pH=5.30, $C_0$=40 mol/m$^3$, v= $0.850\times10^{-4}$ m/sec and L=0.145 m).**

proximately $0.30\text{-}0.80\times10^{-11}$ $m^2/s$.

### 3. Breakthrough Curves under Various Operating Conditions

As a commercial equipment for adsorption separation, a column adsorber has been used since it gives a sharp breakthrough by means of the difference in affinity to the particle. The breakthrough curve of any species in general depends on adsorption equilibrium, interparticle mass transfer, and the hydrodynamic conditions in the column. These factors tend to make the breakthrough curves more dispersive or less sharp. Therefore, it is reasonable to consider adsorption equilibrium and mass transport simultaneously in simulating the adsorption behavior in the fixed-bed adsorber. On the other hand, the operational factors such as input concentration, pH, concentration, flow rate and L/D ratio are important in column designing and optimization. In this work, breakthrough curves were obtained under various experimental conditions mentioned above. The experimental conditions are summarized in Table 3 and corresponding results are shown in Figs. 4-9 together with the predicted curves based on the proposed model. The parameters determined in the previous section were used in these calculations without further adjustment.

Fig. 4 shows the effect of temperature on the adsorption breakthrough curve at two temperatures. As shown in Fig. 1, the adsorption amount at low temperature, 278.15 K was a little higher than that at 298.15 K which generally appeared for physisorption. This fact implies that the adsorption is an exothermic reaction. Thus, the adsorption capacity always decreases with temperature.

There are two difficult problems in the separation of cepalosporin C in its fermentation broths. Firstly, the problem is to remove penicillin N coexisting in broths. Secondly, when the culture becomes older, the filtration is more difficult during the actual operation. It has been known that penicillin N can be destructed at low pH 3.0, at which proteins from the culture medium precipitate. It is necessary to determine the optimum solution pH in order to increase the adsorption capacity to deconstruct penicillin N, and to set fermentation time for the proper filtration. Therefore, it is meaningful to investigate the adsorption capacity and breakthrough behavior at low solution pH. Figs. 5 and 6 represent the effect of pH on breakthrough curves. As shown in Fig. 5 at low solution pH, the adsorption capacity increased but breakthrough curves were becoming abnormal. The proposed model in this study can satisfactorily simulate the experimental breakthrough curve at pH 5.30. However, the predicted curve is in poor agreement with the experimental result at a low pH, 3.40. Fig. 6 shows the experimental breakthrough curves at

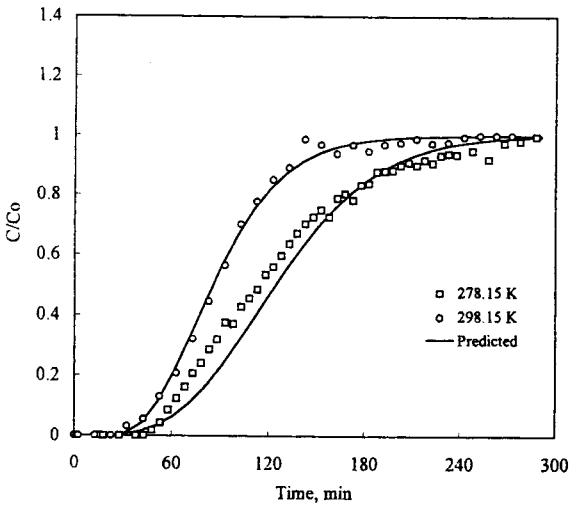


**Fig. 4. Effect of temperature on the experimental results and model predictions of breakthrough curves for adsorption on SP850 (pH=5.30, $C_0$=30 mol/m$^3$, v=$0.531\times10^{-4}$ m/sec and L=0.145 m).**

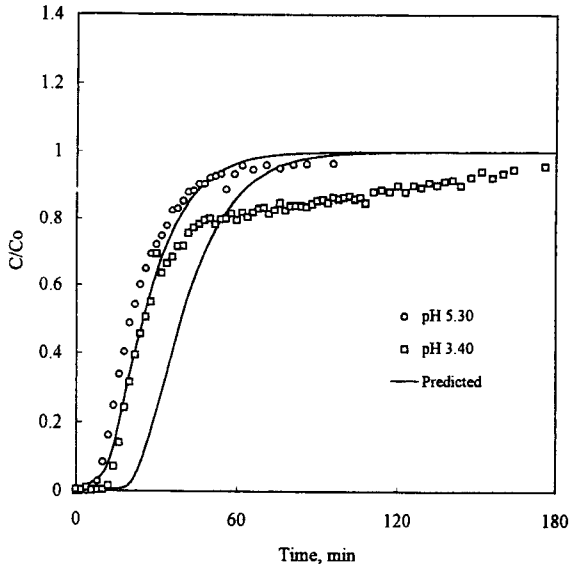


**Fig. 5. Effect of pH on the experimental results and model predictions of breakthrough curves for adsorption on SP850 ($C_0$=40 mol/m$^3$, v=$2.124\times10^{-4}$ m/sec and L=0.145 m).**

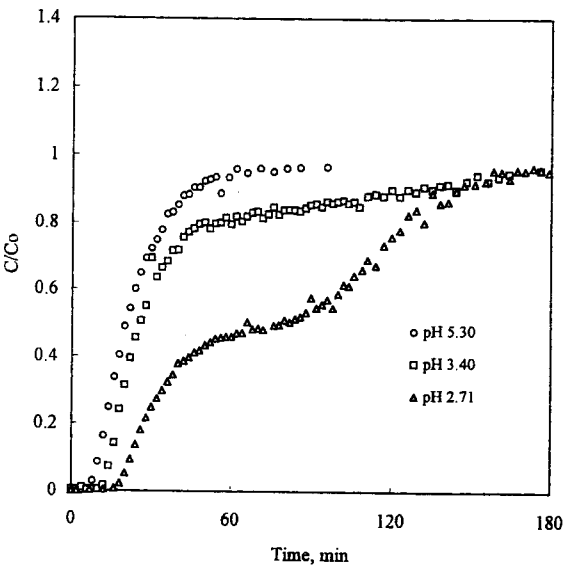


**Fig. 6. Effect of pH on the experimental results and model predictions of breakthrough curves for adsorption on SP850 ($C_0$=40 mol/m$^3$, v=$2.124\times10^{-4}$ m/sec and L=0.145 m).**

pH 5.30, pH 3.40, and pH 2.71 to check the effect of solution pH. The adsorption capacity increased considerably but the breakthrough curve was unusual with decreasing solution pH. These deviations may be due to the fact that cephalosporin C can exist as a mixture of a cation, anion and a neutral ion depending upon the solution pH. Therefore, if we take into account the adsorption equilibria and kinetics on the concept of nonideality in both liquid and adsorbed phases with respect to the individual ion, these deviations can be compensated. This study will be continued systematically.

The dependence of adsorbate concentration on diffusion, is important both in process modeling and in understanding the mechanism of the diffusion process. Several different types of diffusion mechanisms become dominant and sometimes two or three of them compete or cooperate depending on the structure of the adsorbent. The dominant mechanism also depends on adsorbate and adsorbent as well as adsorption conditions such as temperature and concentration. Fig. 7 illustrates the effect of input concentration on experimental breakthrough curves in the concentration range that is usually encountered. The breaktime for higher input concentration is always earlier than that for lower input concentration. The result can be explained by the concept of the moving velocity of the mass transfer zone (MTZ) [Ruthven, 1984], $V_{mtz}$, which is defined as;

$$V_{mtz} = \left(\frac{\partial z}{\partial t}\right)_c = -\frac{(\partial C/\partial t)_z}{(\partial C/\partial z)_t} = \frac{V}{1+\rho_p\left(\frac{1-\varepsilon_b}{\varepsilon_b}\right)\left(\frac{dq^*}{dC}\right)_c} \quad (22)$$

Eq. (22) means that MTZ is a function of interstitial velocity, particle density, bed porosity and $\partial q^*/\partial C$. For a linear isotherm adsorption system, the values of $\partial q^*/\partial C$ is constant with other fixed variables, so that the moving velocity of the MTZ is constant. Therefore the breaktime is not affected by input concentrations. However, the adsorption isotherm of cephalosporin C on SP850 is nonlinear, weakly favorable as shown in Figs. 1 and 2. As the input concentration increases, the value of $\partial q^*/\partial C$ decreases so that the zone velocity increases. Therefore, the breaktime becomes shorter under this circumstance. Further, the shape of the breakthrough curve is somewhat steeper at higher input concentration than that at lower input concentration. This may result from a larger intraparticle diffusivity, because the adsorption zone is reduced by higher diffusion flux. We determined the diffusion coefficient in terms of concentration explicitly, we have done it by fitting the experimental results with model predictions. Thus, these evaluated values stand for the effective surface diffusion coefficients. These values increase with concentration in the range of $0.30\text{-}0.80\times10^{-11}$ $m^2/s$ as shown in Table 5. The effective surface diffusion coefficients were fitted as a function of concentration as follows; $D_s=0.0004C^2+0.0154C+0.752$.

**Table 5. Mass transfer coefficients for cephalosporin C within SP850 at 298.15 K and pH 5.30**

| Conc. [mol/m$^3$] | Flow rate [m/sec] | $k_f\times10^5$ [m/sec] | $D_s\times10^{11}$ [m$^2$/sec] |
|---|---|---|---|
| 12.039 | 0.503 | 1.050 | 0.300 |
| 21.543 | 0.530 | 1.070 | 0.410 |
| 31.281 | 0.503 | 1.050 | 0.500 |
| 38.741 | 0.848 | 1.301 | 0.630 |
| 51.438 | 0.654 | 1.173 | 0.800 |

Since the flow rate is an important factor in column adsorber design, its effect should be checked. Fig. 8 shows that the breaktime appeared earlier with higher flow rate. On the other hand, the breakthrough curves were steeper with

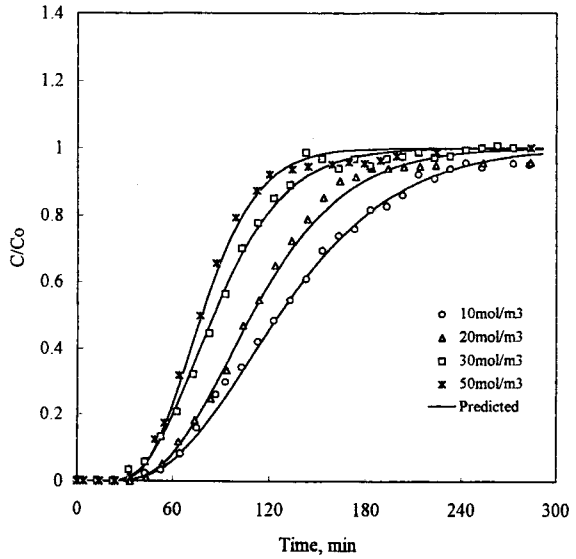


**Fig. 7. Effect of concentration on the experimental results and model predictions of breakthrough curves for adsorption on SP850 (pH=5.30, v=0.531×10$^{-4}$ m/sec and L=0.145 m).**

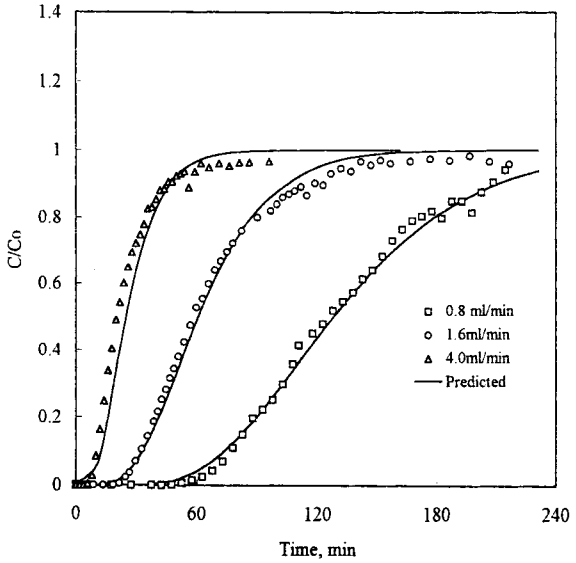


**Fig. 8. Effect of flow rate on the experimental results and model predictions of breakthrough curves for adsorption on SP850 (pH=5.30, $C_0$=40 mol/m$^3$ and L=0.145 m).**

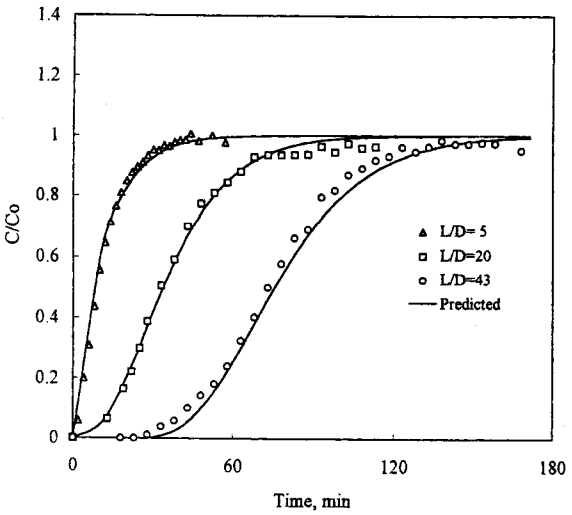


**Fig. 9. Effect of L/D ratio on the experimental results and model predictions of breakthrough curves for adsorption on SP850 (pH=5.30, $C_0$=30 mol/m$^3$ and v=2.124× 10$^{-4}$ m/sec).**

higher flow rate. Since the intraparticle diffusivity is usually independent of flow rate, this was due to the external film mass transfer resistance. This resistance is smaller when flow rate is higher, so that the length of the mass transfer zone is reduced or a sharper breakthrough curve is generated.

When all the other operating conditions are fixed, the breakthrough curves at different column lengths are almost similar. However, Fig. 9 shows the experimental results that the breakthrough curve has a sharper shape for a shorter column. Generally, this results can be observed when the column length is shorter than the zone length. However, the concentration profile in the MTZ becomes a constant pattern after traveling some finite distance, which is usually much longer than the zone length. From our experimental results, the breakthrough curve for L/D=5 is still becoming steeper. However, the constant patterns are formed as increasing L/D ratio toward L/D= 45.

## CONCLUDING REMARKS

As a separation and purification method for cephalosporin C dissolved in aqueous solutions, the adsorption behaviors of cephalosporin C on a nonionic polymeric sorbent, SP850, were investigated in a column adsorber under various operating conditions such as temperature, pH, concentration, flow rate and L/D ratio. Single-species isotherms were well fitted by Langmuir, Freundlich and Sips equations. The adsorption capacity increased with temperature and pH. The axial dispersion coefficient and the film mass transfer coefficient were estimated from experimental conditions by correlations given in literature. The surface diffusion coefficient was obtained from experimental breakthrough data. In this adsorption system, cephalosporin C/SP850, the intraparticle diffusion is highly the rate controlling step. The adsorption model, which employs the surface diffusion for intraparticle mass transfer combined with the Freundlich equation for the single-species equilibrium, successfully simulates the adsorption breakthrough curves under various experimental conditions. However, there were considerable deviations between the experimental results and the model predictions obtained particulary at low solution pHs, since different ionic species may coexist. Therefore, the further work on the effect of pH on adsorption equilibrium and mass transfer rate should be continued.

## ACKNOWLEDGMENT

This research was supported by Korea Science and Engineering Foundation (KOSEF), under Grant No. 941-1100-027-2. The authors gratefully acknowledge the effort of Cheil Food & Chemicals Inc. for supplying the cephalosporin C.

## NOMENCLATURES

AS : collocation coefficient of the first derivative for particles [-]
AF : collocation coefficient of the first derivative for the column [-]
BS : collocation coefficient of the second derivative for particles [-]
BF : collocation coefficient of the second derivative for the column [-]
C : concentration in the fluid phase [mol/m$^3$]
D : column diameter [m]
$D_L$ : axial dispersion coefficient [m$^2$/sec]
$D_m$ : molecular diffusion coefficient [m$^2$/sec]
$D_{si}$ : surface diffusion coefficient [m$^2$/sec]
E : percent error [%]
$k_f$ : film mass transfer coefficient [m/sec]
L : column length [m]
N : number of data point [-]
NC : number of component [-]
NEQ: number of total equations [-]
NF : number of interior collocation points in the column [-]
NS : number of interior collocation points in particles [-]
Pe : Peclet number defined in Eq. (13)
$q_i$ : concentration in particle phase [mol/kg]
r : radial distance [m]
$R_p$ : particle radius [m]
t : time [sec, hr]
T : temperature [K]
z : axial distance [m]
Z : dimensionless bed height [-]

**Greek Letters**

$\alpha$ : dimensionless group
$\beta_i$ : dimensionless group
$\varepsilon_b$ : bed porosity
$\gamma_i$ : dimensionless group
$\lambda_i$ : dimensionless group
$\mu$ : dimensionless group
$\rho_p$ : particle density [kg/m$^3$]
$\tau$ : dimensionless time
v : interstitial velocity [m/sec]

X : dimensionless group
$\xi_i$ : dimensionless concentration in fluid phase
$\Psi_i$ : dimensionless concentration in solid phase

**Superscripts and Subscripts**

i,j,*l* : collocation points
exp : experimental
k : species
pre : predicted
s : interface

**Abbreviation**

conc : concentration
DVB: divinylbenzene
MTZ: mass transfer zone
Re : Reynolds number
Sc : Schmidt number

## REFERENCES


Abraham, E. P., "Biosynthesis of Penicillins and Cephalosporins, in β-Lactam Antibiotics for Clinical Use", Marcel Dekker Inc., New York (1986).

Asenjo, J. A., "Separation Processes in Biotechnology", Marcel Dekker Inc., New York (1983).

Belter, P. A., Cussler, E. L. and Hu, W. S., "Bioseparations, Downstream Processing for Biotechnology", Wiley-Interscience, New York (1988).

Carey, G. F. and Finlayson, B. A., "Orthogonal Collocation on Finite Elements", *Chem. Eng. Sci.*, **30**, 587 (1975).

Costa, C. and Rodriques, A., "Design of Cyclic Fixed-Bed Adsorption Processes. Part I: Phenol Adsorption on Polymeric Adsorbents", *AIChE J.*, **31**, 1645 (1985).

Dechow, F. J., "Sparation and Purification Techniques in Biotechnology", Noyes, Park Ridge, NJ (1989).

Elander, R. P. and Aoki, H., "β-Lactam-Producing Microorganism: Their Biology and Fermentation Behavior, in Chemistry and Biology of β-Lactam Antibiotics", Academic Press, **3**, 83 (1982).

Lee, J. W., Park, H. C. and Moon, H., "Adsorption and Desorption of Cephalosporin C on Non-Ionic Polymeric Sorbents", *Sep. & Purif. Tech.*, (1997) in press

Moon, H. and Lee, W. K., "Intraparticle Diffusion in Liquid-Phase Adsorption of Phenols with Activated Carbon in Finite Batch Adsorber", *J. of Colloid and Interface Science*, **961**, 162 (1983).

Moon, H. and Tien, C., "Further Work on Multicomponent Adsorption Equilibria Calculation Based on the Ideal Adsorbed Solution Theory", *Ind. Eng. Chem. Res.*, **26**, 2042 (1987).

Myers, A. L. and Prausnitz, J. M., "Thermodynamics of Mixed-Gas Adsorption", *AIChE J.*, **11**, 121 (1965).

Nara, K., Ohta, K., Katamoto, K., Mizokami, N. and Fukuda, H., "Method for Separating Cephalosporin C", US Pat. 3 926 973 (1975).

Raghavan, N. S. and Rutheven, D. M., "Numerical Simulation of a Fixed-Bed Adsorption Column by the Method of Orthogonal Collocation", *AIChE J.*, **29**, 922 (1983).

Reid, R. C., Prausnitz, J. M. and Poling, B. E., "The Properties of Gases and Liquids", MaGraw-Hill Co., New York (1994).

Ruthven, D. M., "Principles of Adsorption and Adsorption Processes", John Wiley and Sons, New York (1984).

Smith, A., "Cephalosporins, in Comprehensive Biotechnology", Pergamon Press, **3**, 163 (1985).

Villadsen, J. and Michelsen, M. L., "Solution of Differential Equation Models by Polynomial Approximation", Prentice-Hall, Englewood Cliffs (1978).

Wakao, N. and Funazkri, "Effect of Fluid Dispersion Coefficient on Particle to Fluid Mass Transfer Coefficients in Packed Beds – Correlation of Sherwood Numbers", *Chem. Eng. Sci.*, **33**, 1375 (1978).

Wankat, P. C., "Large-Scale Adsorption Chromatography", CRC Press, Boca Raton, FL (1980).